

Finite-time synchronization of tunnel diode based chaotic oscillators

Patrick Louodop¹, Hilaire Fotsin¹, Michaux Kountchou¹,
Elie B. Megam Ngouonkadi¹, Hilda A. Cerdeira² and Samuel Bowong³

¹ *Laboratory of Electronics and Signal Processing Faculty of Science,
Department of Physics, University of Dschang, P.O. Box 67 Dschang, Cameroon*

² *Instituto de Física Teórica - UNESP, Universidade Estadual Paulista,
Rua Dr. Bento Teobaldo Ferraz 271, Bloco II, Barra Funda, 01140-070 São Paulo, Brazil and*

³ *Laboratory of Applied Mathematics, Department of Mathematics and Computer Science,
Faculty of Science, University of Douala, P.O. Box 24157 Douala, Cameroon*

(Dated: October 17, 2018)

This paper addresses the problem of finite-time synchronization of tunnel diode based chaotic oscillators. After a brief investigation of its chaotic dynamics, we propose an active adaptive feedback coupling which accomplishes the synchronization of tunnel diode based chaotic systems with and without the presence of delay(s), basing ourselves on Lyapunov and on Krasovskii-Lyapunov stability theories. This feedback coupling could be applied to many other chaotic systems. A finite horizon can be arbitrarily established by ensuring that chaos synchronization is achieved at a pre-established time. An advantage of the proposed feedback coupling is that it is simple and easy to implement. Both mathematical investigations and numerical simulations followed by Pspice experiment are presented to show the feasibility of the proposed method.

PACS numbers: 05.45.Xt, 05.45.Jn, 05.45.-a

1. INTRODUCTION

Since chaotic systems were discovered, considerable interest arose in developing and analyzing various systems that exhibit chaos due to their importance in many fields of sciences [1–3]. In biology, epidemiology or in climatology, investigating mathematical models is a part of the strategies used to better comprehend the phenomenon [1, 2, 4, 6–8]. However, there exist difficulties to understand some of them because of the lack of data or the time taken to produce reliable data. For example, in epidemiology, some deceases have to be observed for a long period before they could be modeled [4]. To turn around these problems, electrical circuits (analogue computers) are built to allow the observation of the effect of different parameters. Nevertheless, these electrical circuit have to be synchronized with the time history of data as much as possible to be reliable. Hence, synchronization becomes an important property to be studied.

Another characteristic of synchronization is its applications in chaos based cryptography [9–11]. Even if this problem can be found in a number of papers, most of them deal with infinite settling time [9–11]. If we consider, for example, the application of synchronization in secure communications, the range of time during which the chaotic oscillators are not synchronized corresponds to the range of time during which the encoded message can unfortunately not be recovered or sent. More than a difficulty, this is a catastrophe in digital telecommunications, since the first bits of standardized bit strings always contain signalization data, i.e., the “identity card” of the message. Hence, it clearly appears that

the synchronization time has to be known, minimized, so that the chaotic oscillators synchronize as fast as possible. In this context, it is fair to say that there is a need to study finite-time chaos synchronization. This characteristic is also helpful because of its advantages in its applications in engineering. Hence, it is important to investigate the finite-time stability of nonlinear systems [12–15].

Furthermore, even if delay complicates synchronization, dynamical systems with delay(s) are abundant in nature. They occur in a wide variety of physical, chemical, engineering, economics and biological systems and their networks. There are many examples where delay plays an important role. Some of these examples are listed and presented by M. Lakshamanan and D. V. Senthilkumar in ref. [16]. The mathematical description of delay dynamical systems will naturally involve the delay parameter in some specified way. This can be in the form of differential equations with delay or difference equations with delay and so on [16]. Delay differential equations (DDE) are given in many ways. Again, we refer the reader to ref. [16] for more information.

In telecommunications, the delay notion is inescapable for example because of the relative distance between the transmitter and the receiver. Thus, the use of fast signals is indicated. Presently a solution is provided by electronic components such as tunnel diodes. Developed in 1956 by Léo Esaki, the tunnel diode is a nonlinear device used in very high frequencies amplifiers with low noise and in micro-waves conception. The tunnel diode based sources can provide RF signals above 500 GHz. Fundamental oscillations at 712 GHz from a resonant tunnel diode oscillator were demonstrated by Brown and co-workers in 1991 [17]. Recently, fundamental frequency oscillations of a resonant tunnel diode oscillator close

to (831 GHz, 915 GHz) and above a terahertz (1.04 THz) at room temperature were reported by Suzuki et al. [18] – more details can be found in the PhD thesis of Wang, Liquan (2011) of University of Glasgow [19] and references therein. Considering the frequency capability of the tunnel diode, it can be used as an efficient source for chaotic signals in wireless communications [20]. In particular Hai-Peng Ren et al. show that, for some particular chaotic signals the Lyapunov exponents remain unaltered through multipath propagation, thus making these systems able to sustain communications with chaotic signals. However, experimental observation of generalized synchronization phenomena in microwave oscillators have been done by B. S. Dmitriev et al. [21] and their application to secure communications has been carried out by A. A. Koronovskii et al. [22]. Nevertheless, the synchronization schemes used in the mentioned references [20–22] are dealing with asymptotical synchronization and can only guarantee that two systems achieve synchronization as time tends to infinity, while in real-world applications, one always expects that two systems achieve synchronization within a finite and/or predetermined time. Besides, finite-time synchronization has been confirmed to have better robustness against parametric and external disturbances than the asymptotical one [23, 24]. Hereby the importance to study finite-time synchronization of chaotic systems. The use of tunnel diodes to construct chaotic systems was also reported by A. Pikovskii [25], A. Fradkov [26] and others. For the purpose of this work, we base ourselves on the circuit proposed by A. Fradkov [26] where we replace the used tunnel diode by the one with reference number 1N3858 for which the Pspice model is available in Internet.

In this paper we study an active adaptive finite-time synchronization of tunnel diodes based chaotic oscillators with (first case) and without (second and third cases) time-delay in both the drive and response systems. Therefore, we will investigate the adaptive synchronization of chaotic systems using just one master state variable as output to construct the nonlinear feedback coupling. A robust adaptive response system will be therefore designed to always globally synchronize the given driven tunnel diode based oscillator. These results are of significant interest to infer relationships between nonlinear feedback coupling, time-delay and finite-time synchronization. To the best of our knowledge, this active adaptive finite-time synchronization of chaotic systems using a nonlinear feedback coupling has not yet being reported in the literature.

The manuscript is organized as follows: In section 2, the circuit model and its chaotic dynamics is investigated. Section 3 deals with the adaptive synchronization problem. In this section the active controller is designed and the theoretical settling time in the case of systems without delay is developed. Numerical simulations are per-

formed to show the effectiveness of the synchronization scheme. In section 4, we investigate the cases of delayed systems considering two cases. The theoretical settling is also obtained and the numerical results are presented graphically to prove the effectiveness of the scheme. In the last section we present the conclusions.

2. THE MODEL AND ITS PROPERTIES

Before starting to analyze adaptive synchronization and delay, we introduce the elements of our circuit. Its electronic diagram is given on Fig. (1.a) where the tunnel diode model is the 1N3858 with the current-voltage characteristic given on Fig. (1.b). The chaotic circuit is a R-L-C oscillator where E is a continuous voltage source.

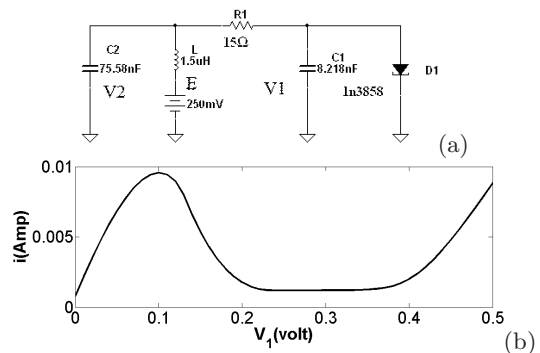


FIG. 1: (a) Circuit diagram and (b) current voltage characteristic of tunnel diode 1N3858.

The circuit diagram presents two capacitors C_1 and C_2 and an inductor L . The nonlinearity is introduced by the tunnel diode which has its current-voltage characteristic depicted in Fig. (1.b). As an approximation of this current-voltage characteristic, we use the following relation [26]:

$$i(V_1) = a_1(V_1 - b)^3 - a_2(V_1 - b) + a_3, \quad (1)$$

where a_1 , a_2 and a_3 are positive constants. The circuit can be described by the following system of differential equations:

$$\begin{cases} \dot{x}_1(\tau) = \alpha[x_2 - x_1 - rf(x_1)], \\ \dot{x}_2(\tau) = \beta(x_1 - x_2 + rx_3), \\ \dot{x}_3(\tau) = \gamma(E - x_2), \end{cases} \quad (2)$$

where

$$\begin{aligned} c &= \frac{C_2}{C_1}, & r &= R_1, & q &= \frac{r}{Lw}, & \tau &= wt, \\ \varrho &= 1V, & I &= 1A, & x_1 &= \frac{V_1}{\varrho}, & x_2 &= \frac{V_2}{\varrho}, \\ x_3 &= \frac{i}{I}, & \alpha &= \frac{c}{q}, \beta = \frac{1}{q}, & \gamma &= \frac{q}{r} & \text{and} \\ f(x_1) &= a_1(x_1 - b)^3 - a_2(x_1 - b) + a_3, \end{aligned}$$

where V_1 and V_2 are the voltages at landmarks of C_1 and C_2 respectively, i is the current which flows through the inductor and w is a constant. Note that Eq. (2) is similar to the so called modified Chua's circuit [27].

Before entering into the description of the system under study we present the chaotic behavior of the circuit due to the influence of parameter α on the evolution of the one-dimensional Lyapunov exponent Fig. (2.a) and on bifurcation diagram Fig. (2.b) These two graphs allow us to determine the value of the control parameter, leading to a chaotic behavior of the system through period doubling. Fig. (2.a) shows that for some values of the parameter α the system Eq. (2) has a positive Lyapunov exponents.

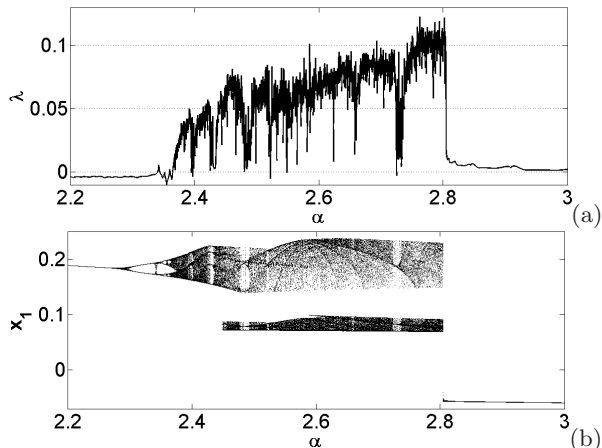


FIG. 2: (a) One dimensional Lyapunov exponent and (b) bifurcation diagram when $E = 0.253208$ and $q = 3.6$.

Figs. (3.a and b) show the graphs x_2 vs x_1 and x_1 vs x_3 obtained from Pspice simulations of the circuit of Fig. (1.a). An approximate behavior is displayed with the following selection of parameters $c = 8.4$, $q = 3.35$, $E = 0.25$, $r = 16$, $a_1 = 1.3242872$, $a_2 = 0.06922314$, $a_3 = 0.005388$ and $b = 0.167$ and initial conditions $x_1(0) = 0.15$, $x_2(0) = 0.27$ and $x_3(0) = 0.008$.

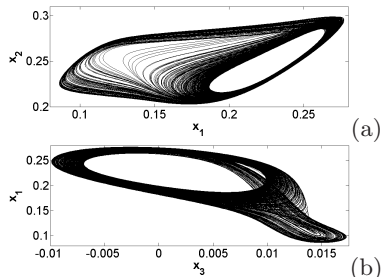


FIG. 3: Chaotic attractor obtained through Pspice simulation of the circuit of Fig.1(a).

In Fig. (4) the space (c, q) for which the system behaves chaotically is shown in black. With $\alpha = 2.507462687$ and the values of the parameters given above, basing ourselves on Fig. 4, it follows that, the Lyapunov expo-

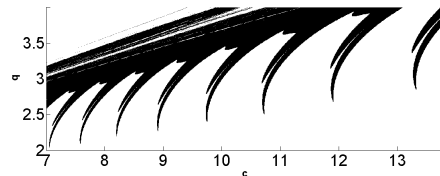


FIG. 4: Pair (c, q) for which chaos occurs with $E = 0.25$.

nent is positive and the system shows chaotic behavior (Fig. 5).

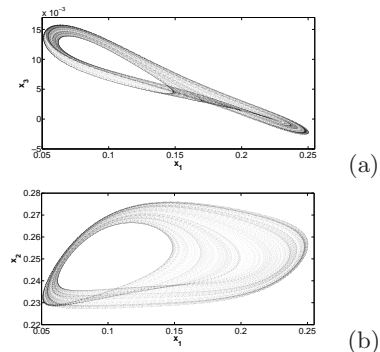


FIG. 5: Chaotic attractor obtained through numerical simulation of Eq. (2).

The graphs of Figs. (6) show the Poincare sections which help to prove the chaotic behavior of the model (Eq. (2)).

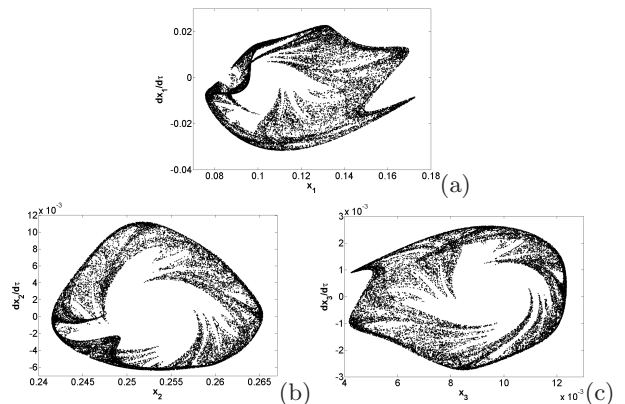


FIG. 6: Poincare sections with $E = 0.253205$, $c = 8.846$ and $q = 3.6$.

3. ADAPTIVE SYNCHRONIZATION

The starting point of the control law design is always a mathematical model of the real system which describes the system response to various control inputs. It is usually assumed that such a model is known rather completely. However, in practice the model describes the real system with some degree of uncertainty. To cope

with this uncertainty in such cases, methods of the adaptive control theory can be employed. The concept of chaos synchronization emerged much later, not until the gradual realization of the usefulness of chaos by scientists and engineers. Chaotic signals are usually broad band and noise-like. Because of these properties, synchronized chaotic systems can be used as cipher generators for secure communication.

In this section, we investigate two identical systems of the type described in the previous section where the system drive $x_i(\tau)$, $i = 1, 2, 3$ drives the response system $y_i(\tau)$, $i = 1, 2, 3$.

3.1. Design of the nonlinear controller

Here we investigate the finite-time synchronization of tunnel diode based chaotic oscillators described by Eq. (2). For this purpose we consider the corresponding response system described by

$$\begin{cases} \dot{y}_1 = \alpha [y_2 - y_1 - rf(y_1)] - \zeta k \operatorname{sign}(y_1 - x_1) - \zeta u(\tau), \\ \dot{y}_2 = \beta [y_1 - y_2 + ry_3 - 2(y_1 - x_1)], \\ \dot{y}_3 = \gamma (E - y_2), \end{cases} \quad (3)$$

where k and ζ are positive constant gains to be defined by the designer. The term $-2(y_1 - x_1)$ added in the y_2 -axis stabilizes the slave system. The nonlinear controller is expressed as $-\zeta k \operatorname{sign}(y_1 - x_1) - \zeta u(\tau)$ where $u(\tau)$ is the adaptive feedback coupling designed to achieve finite-time synchronization. All parts of the used controller contribute to synchronize both drive-response systems at an established time and also to stabilize the response dynamics.

Let us define the synchronization error as follows

$$e_i(\tau) = y_i(\tau) - x_i(\tau), \quad \text{with} \quad i = 1, 2, 3. \quad (4)$$

Subtracting Eq. (2) from Eq. (3) and using Eq. (4), we obtain:

$$\begin{cases} \dot{e}_1 = \alpha [e_2 - e_1 - \phi_0(x_1, y_1)] - \zeta k \operatorname{sign}(e_1) - \zeta u(\tau), \\ \dot{e}_2 = \beta [-e_1 - e_2 + re_3], \\ \dot{e}_3 = -\gamma e_2, \end{cases} \quad (5)$$

where $\phi_0(x_1, y_1) = r(f(y_1) - f(x_1))$.

The synchronization problem can be stated as follows: considering the transmitter Eq. (2) and the receiver Eq. (3) with any initial conditions, $e_1(0) = y_1(0) - x_1(0)$, $e_2(0) = y_2(0) - x_2(0)$, $e_3(0) = y_3(0) - x_3(0)$, it is our aim to design the form of the function $u(\tau)$ which synchronizes the orbits of both the transmitter and the response

systems and thus provides the stabilization of Eq. (5) at an established finite-time τ_s , i.e.,

$$\begin{aligned} \lim_{t \rightarrow \tau_s} x_i(\tau) &= y_i(\tau), \quad i = 1, 2, 3, \\ \lim_{\tau \rightarrow \tau_s} \|e(\tau)\| &= 0. \end{aligned} \quad (6)$$

where τ_s is the settling time. We consider that, the function $\phi_0(x_1, y_1)$ respects the Lipschitz condition. I.e., it exists a positive constant χ_0 such that $|\phi_0(x_1, y_1)| \leq \chi_0 |e_1(\tau)|$.

3.2. Main results

The global finite-time synchronization is achieved when the Lyapunov function candidate is proper [15], namely, the time derivative of the used Lyapunov function is bounded by a negative constant.

Let us consider the following candidate for the Lyapunov function [28]

$$V = \frac{1}{2} \left(\frac{e_1^2}{\alpha} + \frac{e_2^2}{\beta} + \frac{re_3^2}{\gamma} \right) + |u(\tau)|. \quad (7)$$

The time derivative along the trajectories of the system of Eqs. (5) yields

$$\begin{aligned} \dot{V} &= -e_1^2 - e_2^2 - \phi_0(x_1, y_1)e_1 - \frac{\zeta k}{\alpha} |e_1| - \frac{\zeta u(\tau)}{\alpha} e_1 \\ &\quad + \operatorname{sign}(u)\dot{u}(\tau), \\ &\leq -e_1^2 - e_2^2 + |\phi_0(x_1, y_1)||e_1| - \frac{\zeta k}{\alpha} |e_1| - \frac{\zeta u(\tau)}{\alpha} e_1 \\ &\quad + \operatorname{sign}(u)\dot{u}(\tau), \\ &\leq -(1 - \chi_0)e_1^2 - e_2^2 - \frac{\zeta k}{\alpha} |e_1| - \frac{\zeta u(\tau)}{\alpha} e_1 \\ &\quad + \operatorname{sign}(u)\dot{u}(\tau). \end{aligned} \quad (8)$$

Letting $\chi_0 < 1$ and $\zeta = \alpha$,

$$\dot{V} \leq -k|e_1| - u(\tau)e_1 + \operatorname{sign}(u)\dot{u}(\tau). \quad (9)$$

Considering the finite-time stability theory applied in [15], it follows that, there exists a certain positive constant p such that the following relation yields

$$\dot{V} \leq -p. \quad (10)$$

If the objective is reached, the theoretical finite-time for synchronization is obtained by integrating Eq. (10) from 0 to τ_s . Thus, one has

$$\tau_s \leq \frac{1}{2p} \left(\frac{e_1^2(0)}{\alpha} + \frac{e_2^2(0)}{\beta} + \frac{re_3^2(0)}{\gamma} \right) + \frac{|u(0)|}{p}. \quad (11)$$

Therefore, in accordance with Eq. (10), the controller $u(\tau)$ is designed through the following relation

$$\dot{u} = \text{sign}(u) (k|e_1| + ue_1 - p), \quad (12)$$

and we construct the slave system Eq. (3) as follows

$$\begin{cases} \dot{y}_1 = \alpha [y_2 - y_1 - rf(y_1)] - \zeta k \text{sign}(y_1 - x_1) - \zeta u, \\ \dot{y}_2 = \beta [y_1 - y_2 - ry_3 - 2(y_1 - x_1)], \\ \dot{y}_3 = \gamma [E - y_2], \\ \dot{u} = \text{sign}(u) (k|e_1| + ue_1 - p). \end{cases} \quad (13)$$

3.3. Numerical results

To illustrate the effectiveness of the proposed scheme we present some numerical results for the initial conditions given by $(x_1(0), x_2(0), x_3(0)) = (0.15, 0.27, 0.008)$ and $(y_1(0), y_2(0), y_3(0)) = (-0.15, -0.27, -0.008)$, the parameters $p = 0.001$, $k = 0.005$ and the initial condition of controller $u(0) = 0.0001$. The integration time step was taken as 10^{-4} . For such values, the theoretical settling time is determined to be $\tau_{sTH} = 521.0579$. The graphs of Fig. (7) show the time dependence of the master system state variables (solid lines) and the corresponding slave system state variables (dashed lines). From the graphs in Fig. (8) we confirm that the

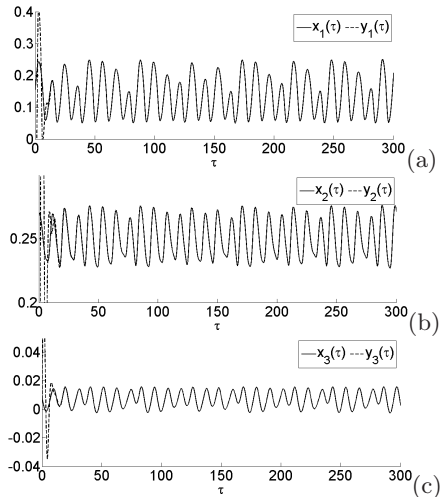


FIG. 7: Time histories of state variables, solid line for drive system and dashed line for response system.

synchronization is reached in finite-time. It is observed that synchronization is reached at time $\tau_{sNU} \simeq 245.3$ which respects the finite-time condition $\tau_{sNU} \leq \tau_{sTH}$ (See Fig. (8b)).

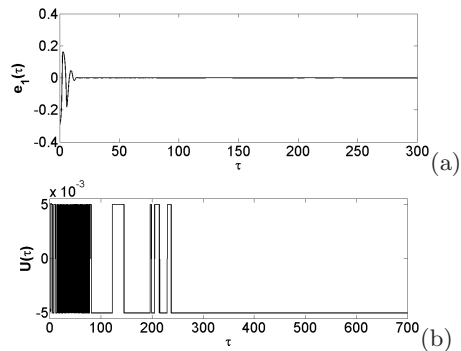


FIG. 8: Time histories of $e_1(\tau)$ (a) and of the controller $u(\tau)$ (b).

The value of the finite-time of stability depends strongly on the values of parameters p . Considering $k \simeq 0.005$ the following graphs represent the behavior of the error state $e_1(\tau)$ and of the adaptive parameter $u(\tau)$ for two given values of p (Fig. (9.a)). In principle p can take any values, but to deal with finite-time stability, it should be small. The graphs in Fig. (9) represent the behavior of both $e_1(\tau)$ and $u(\tau)$ for $p = 0.0017$ and $p = 0.002$ (See Figs. (9)(a) and (b) and Figs. (9)(c) and (d) respectively). In this paper we define the numerical finite-time of convergence as the end time of the transitory phase of the time evolution of $e_1(\tau)$. For the graphs on Fig. (9a) and Fig. (9b) the numerical finite-time is $\tau_{sNU} \simeq 100$ and the theoretical finite-time is $\tau_{sTH} \simeq 306.5047$ while for the ones on Fig. (9c) and Fig. (9d) the theoretical finite-time is $\tau_{sTH} \simeq 260.5290$ and the numerical finite-time $\tau_{sNU} > \tau_{sTH}$. Thus we see that the finite-time condition $\tau_{sNU} \leq \tau_{sTH}$ is fulfilled in both cases.

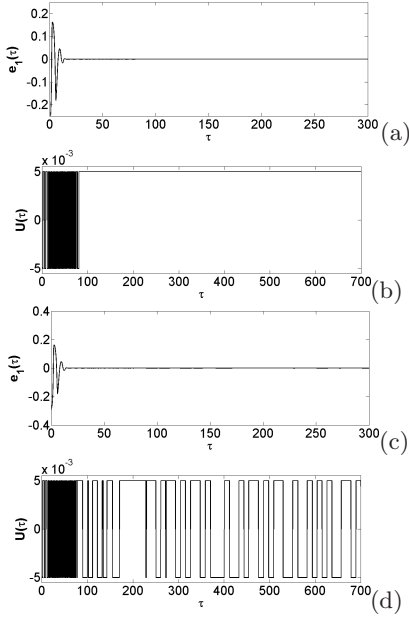


FIG. 9: Behaviors of $e_1(\tau)$ and $u(\tau)$. Figs.(a) and (b): $p = 0.0017$. Figs.(c) and (d): $p = 0.02$.

4. FINITE-TIME TIME-DELAY SYNCHRONIZATION OF CDT

4.1. Systems with internal delay

4.1.1. Synchronization analysis

In this section, we investigate the finite-time synchronization of delayed tunnel diode based chaotic oscillators. We first consider the presence of one delay affecting the nonlinearity of each drive system and response system. Thus, the master and slave systems become respectively

$$\begin{cases} \dot{x}_1(\tau) = \alpha[x_2 - x_1 - rf(x_1(\tau - \theta))], \\ \dot{x}_2(\tau) = \beta(x_1 - x_2 + rx_3), \\ \dot{x}_3(\tau) = \gamma(E - x_2), \end{cases} \quad (14)$$

and

$$\begin{cases} \dot{y}_1 = \alpha[y_2 - y_1 - rf(y_1(\tau - \theta)) \\ \quad - \zeta k \operatorname{sign}(y_1 - x_1) - \zeta u(\tau)], \\ \dot{y}_2 = \beta[y_1 - y_2 + ry_3 - 2(y_1 - x_1)], \\ \dot{y}_3 = \gamma[E - y_2], \end{cases} \quad (15)$$

where θ is the time-delay.

For such a case, we define the functions $\phi_1(x_1(\tau - \theta), y_1(\tau - \theta)) = r(f(y_1(\tau - \theta)) - f(x_1(\tau - \theta)))$ and $e_1(\tau - \theta) = y_1(\tau - \theta) - x_1(\tau - \theta)$. Thus the error state is given by the following set of equations

$$\begin{cases} \dot{e}_1 = \alpha[e_2 - e_1 - \phi_1(x_1(\tau - \theta), y_1(\tau - \theta))] \\ \quad - \zeta k \operatorname{sign}(e_1) - \zeta u(\tau), \\ \dot{e}_2 = \beta[-e_1 - e_2 + re_3], \\ \dot{e}_3 = -\gamma e_2, \end{cases} \quad (16)$$

From here, using the same controller as in the previous section, we choose the following Krasovskii-Lyapunov function candidate [28, 31]:

$$\begin{aligned} V = & \frac{1}{2} \left(\frac{e_1^2}{\alpha} + \frac{e_2^2}{\beta} + \frac{re_3^2}{\gamma} \right) + |u(\tau)| \\ & + \eta \int_{-\theta}^0 e_1^2(\tau + s) ds, \end{aligned} \quad (17)$$

where η is a positive constant to be determined.

The time derivative along the trajectories of the system Eq. (16) yields

$$\begin{aligned} \dot{V} = & -(1 - \eta)e_1^2 - e_2^2 - \phi_1(\tau - \theta)e_1 - \frac{\zeta k}{\alpha}|e_1| \\ & - \frac{\zeta u(\tau)}{\alpha}e_1 + \operatorname{sign}(u)\dot{u}(\tau) - \eta e_1^2(\tau - \theta), \\ \leq & -(1 - \eta)e_1^2 - e_2^2 + |\phi_1(\tau - \theta)||e_1| - \frac{\zeta k}{\alpha}|e_1| \\ & - \frac{\zeta u(\tau)}{\alpha}e_1 + \operatorname{sign}(u)\dot{u}(\tau) - \eta e_1^2(\tau - \theta). \end{aligned} \quad (18)$$

Let assume that $|\phi_1(\tau - \theta)| \leq \chi_1|e_1(\tau - \theta)|$, where χ_1 is a positive constant. It follows from here that

$$\begin{aligned} \dot{V} \leq & -e_1^2 - e_2^2 + \chi_1|e_1(\tau - \theta)||e_1| - \frac{\zeta k}{\alpha}|e_1| - \frac{\zeta u(\tau)}{\alpha}e_1 \\ & + \operatorname{sign}(u)\dot{u}(\tau) + \eta e_1^2 - \eta e_1^2(\tau - \theta), \\ \dot{V} \leq & -\left(1 - \frac{\chi_1}{2} - \eta\right)e_1^2 - e_2^2 + \left(\frac{\chi_1}{2} - \eta\right)e_1^2(\tau - \theta) \\ & - \frac{\zeta k}{\alpha}|e_1| - \frac{\zeta u(\tau)}{\alpha}e_1 + \operatorname{sign}(u)\dot{u}(\tau). \end{aligned} \quad (19)$$

Let $\eta = \frac{\chi_1}{2}$, $\chi_1 < 1$ and $\zeta = \alpha$, it follows that

$$\dot{V} \leq -k|e_1| - u(\tau)e_1 + \operatorname{sign}(u)\dot{u}(\tau). \quad (20)$$

Thus, using the following controller

$$\dot{u} = \operatorname{sign}(u)(k|e_1| + ue_1 - p), \quad (21)$$

it follows that

$$\dot{V} \leq -p. \quad (22)$$

Hence, global finite-time stability is achieved [15]. For any time τ contained in the interval $0 < \tau < \theta$ both the

drive and response system do not oscillate at the considered regime. Therefore, to determine the theoretical finite settling time, we integrate Eq. (22) from θ to τ_s and we obtain:

$$V(\tau_s) - V(\theta) \leq -p(\tau_s - \theta). \quad (23)$$

Using the fact that $V(\tau_s) \rightarrow 0$ when $\tau \rightarrow \tau_s$, $V > 0 \forall \tau$ and taking into account Eq. (22), we can see that the Lyapunov function V is a monotonous and decreasing function, it follows that

$$\begin{aligned} \tau_s &= \theta + \frac{1}{2p} \left(\frac{1}{\alpha} e_1^2(\theta) + \frac{1}{\beta} e_2^2(\theta) + \frac{R}{\gamma} e_3^2(\theta) \right) + \frac{|u(\theta)|}{p} \\ &\quad + \eta \int_{-\theta}^0 \varepsilon_1^2(\theta + s) ds, \\ &\geq \theta + \frac{1}{2p} \left(\frac{1}{\alpha} e_1^2(\theta) + \frac{1}{\beta} e_2^2(\theta) + \frac{R}{\gamma} e_3^2(\theta) \right) + \frac{|u(\theta)|}{p}. \end{aligned} \quad (24)$$

Eq. (24) gives the maximum settling time for synchronization. Hence, the finite-time synchronization is reached when the numerical settling time τ_{sNU} satisfies the relation $\tau_{sNU} < \tau_{sTH}$, where $\tau_{sTH} = \theta + \frac{1}{2p} \left(\frac{1}{\alpha} e_1^2(\theta) + \frac{1}{\beta} e_2^2(\theta) + \frac{R}{\gamma} e_3^2(\theta) \right) + \frac{|u(\theta)|}{p}$.

4.1.2. Numerical results

In this section we investigate the finite-time synchronization of two delayed tunnel diode based chaotic systems basing ourselves on the obtained numerical results of the established theory in the previous subsection. The integration time step taken was 10^{-4} . Fig. (10) helps to confirm the synchronization behavior of both delayed master system (Eq. (14)) and slave system (Eq. (15)) when $p = 0.001$ and $k = 0.005$. With this selected values of parameters p and k , the theoretical settling time results $\tau_{sTH} \simeq 127.5448$, while the numerical settling time corresponding to the condition given before is $\tau_{sNU} \simeq 99.4$.

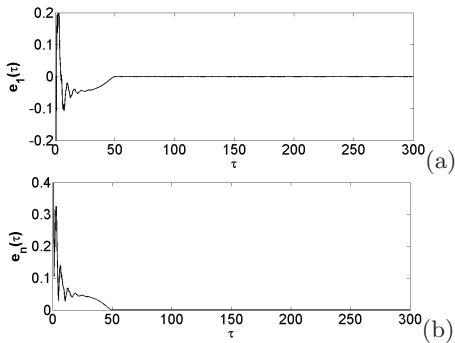


FIG. 10: Time history of $e_1(\tau)$ (a) and $e_n(\tau) = \sqrt{e_1^2(\tau) + e_2^2(\tau) + e_3^2(\tau)}$ (b).

When varying the time-lag θ , just the theoretical settling time is modified when synchronization occurs and the numerical finite-time is determined as $\tau_{sNU} \simeq 99.4$.

4.2. Multi-delayed systems

4.2.1. Synchronization analysis

In this section we consider that there exist two delays: θ_1 represents the time-lag taken for the introduction of the nonlinearity and θ_2 being the time-delay between the master state and the slave state. Thus, the systems become:

$$\begin{cases} \dot{x}_1(\tau - \theta_2) = \alpha[x_2(\tau - \theta_2) - x_1(\tau - \theta_2) \\ \quad - rf(x_1(\tau - \theta_1 - \theta_2))], \\ \dot{x}_2(\tau - \theta_2) = \beta(x_1(\tau - \theta_2) - x_2(\tau - \theta_2) \\ \quad + rx_3(\tau - \theta_2)), \\ \dot{x}_3(\tau - \theta_2) = \gamma(E - x_2(\tau - \theta_2)), \end{cases} \quad (25)$$

and

$$\begin{cases} \dot{y}_1(\tau) = \alpha[y_2(\tau) - y_1(\tau) - rf(y_1(\tau - \theta_1))] \\ \quad - \zeta k \text{sign}(y_1(\tau) - x_1(\tau - \theta_2)) - \zeta u(\tau), \\ \dot{y}_2(\tau) = \beta[y_1(\tau) - y_2(\tau) + ry_3 - 2(y_1(\tau) - x_1(\tau - \theta_2))], \\ \dot{y}_3(\tau) = \gamma[E - y_2(\tau)]. \end{cases} \quad (26)$$

In this case, we define the functions $\phi_2(\tau, \theta_1, \theta_2) = r(f(y_1(\tau - \theta_1)) - f(x_1(\tau - \theta_1 - \theta_2)))$ and $e_1(\tau - \theta_1 - \theta_2) = y_1(\tau - \theta_1) - x_1(\tau - \theta_1 - \theta_2)$. Thus the error state is given by the following set of equations

$$\begin{cases} \dot{e}_1 = \alpha[e_2 - e_1 - \phi_2(\tau, \theta_1, \theta_2) \\ \quad - \zeta k \text{sign}(e_1) - \zeta u(\tau)], \\ \dot{e}_2 = \beta[-e_1 - e_2 + re_3], \\ \dot{e}_3 = -\gamma e_2, \end{cases} \quad (27)$$

Let us now select the Krasovskii-Lyapunov function as [28, 31]:

$$\begin{aligned} V &= \frac{1}{2} \left(\frac{e_1^2}{\alpha} + \frac{e_2^2}{\beta} + \frac{re_3^2}{\gamma} \right) + |u(\tau)| \\ &\quad + \lambda \int_{-\theta_1}^0 e_1^2(\tau - \theta_2 + s) ds, \end{aligned} \quad (28)$$

where λ is a positive constant to be determined. The time derivative along the trajectories of the system Eq. (27) yields

4.2.2. Numerical results

$$\begin{aligned}
\dot{V} &= -(1-\lambda)e_1^2 - e_2^2 - \phi_2(\tau, \theta_1, \theta_2)e_1 - \frac{\zeta k}{\alpha}|e_1| \\
&\quad - \frac{\zeta u(\tau)}{\alpha}e_1 + \text{sign}(u)\dot{u}(\tau) - \lambda e_1^2(\tau - \theta_1 - \theta_2), \\
&\leq -(1-\lambda)e_1^2 - e_2^2 + |\phi_2(\tau, \theta_1, \theta_2)||e_1| - \frac{\zeta k}{\alpha}|e_1| \\
&\quad - \frac{\zeta u(\tau)}{\alpha}e_1 + \text{sign}(u)\dot{u}(\tau) - \lambda e_1^2(\tau - \theta_1 - \theta_2). \tag{29}
\end{aligned}$$

Let assume that $|\phi_2(\tau, \theta_1, \theta_2)| \leq \chi_2|e_1(\tau - \theta_1 - \theta_2)|$, where χ_2 is positive constant. It follows from here that

$$\begin{aligned}
\dot{V} &\leq -e_1^2 - e_2^2 + \chi_2|e_1(\tau - \theta_1 - \theta_2)||e_1| - \frac{\zeta k}{\alpha}|e_1| \\
&\quad - \frac{\zeta u(\tau)}{\alpha}e_1 + \text{sign}(u)\dot{u}(\tau) + \lambda e_1^2 - \lambda e_1^2(\tau - \theta_1 - \theta_2), \\
\dot{V} &\leq -\left(1 - \frac{\chi_2}{2} - \lambda\right)e_1^2 + \left(\frac{\chi_2}{2} - \lambda\right)e_1^2(\tau - \theta_1 - \theta_2) \\
&\quad - \frac{\zeta k}{\alpha}|e_1| - e_2^2 - \frac{\zeta u(\tau)}{\alpha}e_1 + \text{sign}(u)\dot{u}(\tau). \tag{30}
\end{aligned}$$

Let $\lambda = \frac{\chi_2}{2}$, $\chi_2 < 1$ and $\zeta = \alpha$, it follows that

$$\dot{V} \leq -k|e_1| - u(\tau)e_1 + \text{sign}(u)\dot{u}(\tau). \tag{31}$$

Thus, using the following controller Eq. (32),

$$\dot{u} = \text{sign}(u)(k|e_1| + ue_1 - p), \tag{32}$$

it follows that

$$\dot{V} \leq -p. \tag{33}$$

Hence, the global finite-time stability is achieved [15]. When $0 < \tau < \theta_1 + \theta_2$ the system can not oscillate at the considered regime. In order to determine the theoretical finite settling time, we integrate the Eq. (33) from $\theta_1 + \theta_2$ to τ_s . Thus, the finite settling time is given by:

$$\begin{aligned}
\tau_s &= \frac{1}{2p} \left(\frac{1}{\alpha}e_1^2(\theta_1 + \theta_2) + \frac{1}{\beta}e_2^2(\theta_1 + \theta_2) + \frac{R}{\gamma}e_3^2(\theta_1 + \theta_2) \right) \\
&\quad + \frac{|u(\theta_1 + \theta_2)|}{p} + \lambda \int_{-\theta_1 + \theta_2}^0 \epsilon_1^2(\theta_1 + \theta_2 + s) ds + \theta_1 + \theta_2, \\
&\geq \frac{1}{2p} \left(\frac{1}{\alpha}e_1^2(\theta_1 + \theta_2) + \frac{1}{\beta}e_2^2(\theta_1 + \theta_2) + \frac{R}{\gamma}e_3^2(\theta_1 + \theta_2) \right) \\
&\quad + \frac{|u(\theta_1 + \theta_2)|}{p} + \theta_1 + \theta_2. \tag{34}
\end{aligned}$$

At this moment, as in the previous section, the finite-time synchronization is reached when the numerical settling time τ_{sNU} satisfies the relation $\tau_{sNU} < \tau_{sTH}$, where

$$\begin{aligned}
\tau_{sTH} &= \frac{1}{2p} \left(\frac{1}{\alpha}e_1^2(\theta_1 + \theta_2) + \frac{1}{\beta}e_2^2(\theta_1 + \theta_2) + \frac{R}{\gamma}e_3^2(\theta_1 + \theta_2) \right) \\
&\quad + \frac{|u(\theta_1 + \theta_2)|}{p} + \theta_1 + \theta_2.
\end{aligned}$$

From our investigations, it comes out that, the finite-time synchronization is hardly reached when we consider that both dynamics of the drive system and response system are subjected to delay θ_2 . The integration time step used in this part was 10^{-4} . The following graphs on Fig. (11) show that the goal could be achieved only if θ_2 is relatively small. For the following values $k = 0.005$, $p = 0.001$, $\theta_1 = 0.1$ and $\theta_2 = 0.0003$, one has the following behavior.

Considering the behavior of the synchronization error

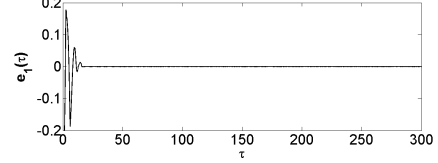


FIG. 11: Time history of $e_1(\tau)$.

$e_1(\tau)$ and $e_n(\tau)$ (defined in Fig. (10)), one can observe the destruction of the synchronization when we increase the value of θ_2 (See Figs. (12), Figs. (13) and Figs. (14)).

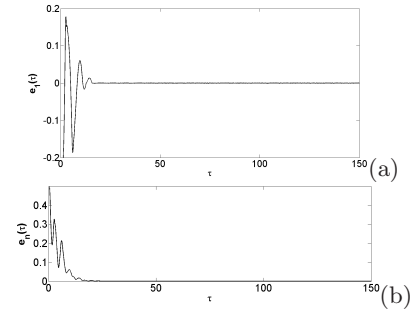


FIG. 12: Time history of (a) $e_1(\tau)$ and (b) $e_n(\tau)$ when $\theta_2 = 0.0003$.

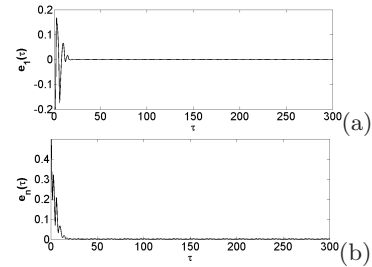


FIG. 13: Time history of (a) $e_1(\tau)$ and (b) $e_n(\tau)$ when $\theta_2 = 0.004$.

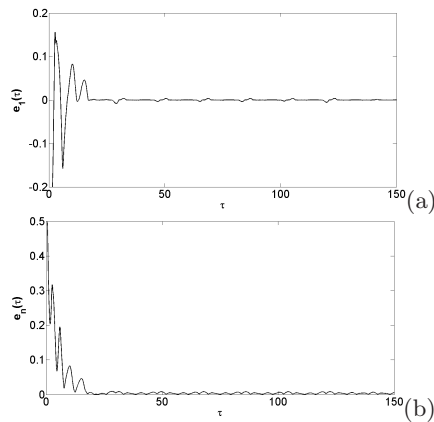


FIG. 14: Time history of (a) $e_1(\tau)$ and (b) $e_n(\tau)$ when $\theta_2 = 0.08$.

5. CONCLUSIONS

The target of this paper was to investigate the possibility to achieve synchronization in finite-time of two tunnel diode based chaotic oscillators. We have considered the case of chaotic systems without and with delay (internal delay and multiple delays). The controller was built basing ourselves on the absolute stability theory [28] and on the Krasovskii-Lyapunov stability theory [31]. Later, the expression of the settling finite-time was investigated in all considered cases. Numerical simulations were performed and given to confirm our theoretical analysis. We observe that the finite-time synchronization was reached when some conditions, which are given and proved by numerical results, are filled.

-
- [1] B. Blasius, A. Huppert and L. Stone, *Nature* **399**, 354 (1999).
- [2] D. W. Graham, C. W Knapp, E. S Van Vleck, K. Bloor, Teresa B. Lane and C. E. Graham, *Int. Soc. Microb. Ecol. J.* **1**, 385 (2007).
- [3] P. Louodop, H. Fotsin and S. Bowong, *Phys. Scr.* **85**, 025002 (2012).
- [4] S. Bowong and J. Kurths, *Phys. Lett. A* **374**, 4496 (2010).
- [5] A. Casadevall, f. C. Fang, L-a. Pirofski, *PLoS Pathog* **7** 1002136 (2011).
- [6] P. Philippe, *Hum. Biol.* **65**, 525 (1993).
- [7] D. J. D. Earn, P. Rohanian and B. Y. Grenfell, *Proc R. Soc. Lond. B* **265**, 7 (1998).
- [8] E. Beninca, J. Huisman, R Heerkloss, K. D. Johnk, P. Branco, E. H. van Nes, M. Scheffer and S. P. Ellner, *Nature* **451**, 822 (2008).
- [9] C. Cruz-Hernandez, *Nonlinear Dynamics and Systems Theory* **1**, 1 (2004).
- [10] S. Bowong and J.J. Tewa, *Math. Comput. Model.* **48**, 1826 (2008).
- [11] M. Feki, *Chaos Solitons Fractals* **18**, 141 (2003).
- [12] W. Yang, X. Xia, Y. Dong and S. Zheng, *Computer and Information Science* **3** 174 (2010).
- [13] Z. Gui, X. Wu and Q. Lin, in *Proceedings of the 2009 International Workshop on Chaos-Fractals Theories and Applications*, 2009, (Ieee Computer Society Washington, DC, USA, 2009),p.16.
- [14] M. P. Lazarevi and D. Lj. Debeljkovi, *Asian J. Control* **7**, 440 (2005).
- [15] L. A. Zuppa, C. C. Hernández and A. Y. A. Bustos, Finite synchronization of Lorenz-based chaotic systems, 2002, <http://www.wseas.us/e-library/conferences/mexico2002/papers/249.pdf>.
- [16] M. Lakshmanan, D. V. Senthilkumar, *Dynamics of Non-linear time-delay systems*(Springer-verlag, New York, 2010).
- [17] E. R. Brown, J. R. Soderstrom, C. D. Parker, L. J. Mahoney, K. M. Molvar and T. C. McGill, *Appl. Phys. Lett.* **58**, 2291 (1991).
- [18] S. Suzuki, A. Teranishi, K. Hinata, M. Asada, H. Sugiyama and H. Yokoyama, *Appl. Phys. Express.* **58**, 192 (2009).
- [19] L. Wang, *Reliable design of tunnel diode and resonant tunnelling diode based microwave sources. PhD thesis*(Glasgow University, 2011, <http://theses.gla.ac.uk/3423/>).
- [20] H. Ren, M. S. Baptista and C. Grebogi, *Physical Review Letters* **110**, 184101-1 (2013).
- [21] B. S. Dmitriev, A. E. Hramov, A. A. Koronovskii, A. V. Starodubov, D. I. Trubetskov and Y. D. Zharkov, *Physical Review Letters* **102** 074101-1 (2009).
- [22] A. A. Koronovskii, O. I. Moskalenko, A. E. Hramov, *Physics-Uspexhi* **52**, 1213 (2009).
- [23] Y. Liu, *Nonlinear Dynamics* **67**, 89 (2012).
- [24] H. Wang, Z. Han, Q. Xie, W. Zhang, *Nonlinear Analysis: Real World Applications* **10**, 2842 (2009).
- [25] A. S. Pikovskii and M. I. Rabinovich, *Sov. Phys. Dokl.* **23**, 183 (1978).
- [26] A. Y. Markov, A. L. Fradkov and G. S. Simin, in *Proceeding of 35th Conference on Decision and Control*, 1996,(Kobe, 1996),p.2177.
- [27] M. T. Yassen, *Appl. Math. Comput.* **135**, 113 (2003).
- [28] X. Liao and P. Yu, *Absolute stability of nonlinear control systems*(Springer science + Buisness Media B. V, New York, 2008).
- [29] J. C. Sprott, *Phys. Lett. A* **266**, 19 (2000).
- [30] J. Lin, C. Huang, T. Liao and J. Yan, *Digit. Signal Process.* **20**, 229 (2010).
- [31] D. V. Senthilkumar, J. Kurths and M. Lakshmanan, *Phys. Rev. E* **79**, 066208 (2009).

Appendx: Circuit design and simulations

Here we investigate the electrical circuit of the system. First we build the analogue computer of the chaotic oscillator, which is shown in Fig. (15). The use of the analogue computer here is helpful because we can modify the frequency of the oscillator and thus facilitate the design of the controller.

This circuit is obtained through the following relations:

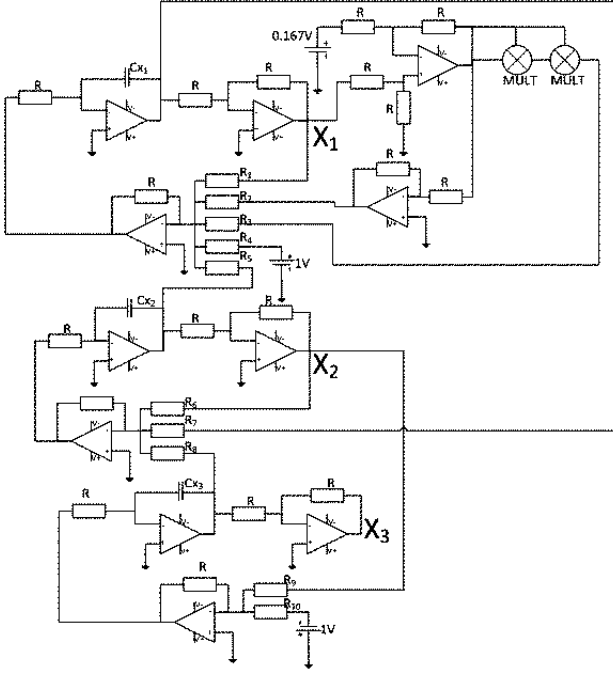


FIG. 15: Circuit diagram of the analogue CDT system.

$\alpha = \frac{1}{\chi R_1 C_{x_1}} = \frac{1}{\chi R_5 C_{x_1}}$, $\alpha r a_1 = \frac{1}{\chi R_3 C_{x_1}}$, $\alpha r a_2 = \frac{1}{\chi R_2 C_{x_1}}$, $\alpha r a_3 = \frac{1}{\chi R_4 C_{x_1}}$, $\beta = \frac{1}{\chi R_7 C_{x_2}} = \frac{1}{\chi R_6 C_{x_2}}$, $\beta r = \frac{1}{\chi R_8 C_{x_2}}$, $\gamma = \frac{1}{\chi R_9 C_{x_3}}$ and $\gamma E = \frac{1}{\chi R_{10} C_{x_3}}$ where χ is a parameter chosen as $\chi = 10^4$. Thus, considering that $R = 10k\Omega$ and all capacitors are $C = 10nF$, we obtain the following components values $R_1 = R_5 = 3988.095238\Omega$, $R_3 = 188.2189546\Omega$, $R_2 = 3.48k\Omega$, $R_4 = 46261.31262\Omega$, $R_6 = R_7 = 33.5k\Omega$, $R_8 = 2093.75\Omega$, $R_9 = 47761.19403\Omega$ and $R_{10} = 191044.7761\Omega$. The chaotic behavior of the above circuit is given by the graphs of the following Fig. (16).

Later on the drive (Fig. (17)) and response (Fig. (18)) systems are designed as follows: The controller (See Fig. (19)) is designed using the following parameters: $2\beta = \frac{1}{\chi R_{C_1} C_{y_2}}$, $\zeta k = \frac{1}{\chi R_{C_2} C_{y_1}}$, $\zeta = \frac{1}{\chi R_{C_3} C_{y_1}}$, $k = \frac{1}{\chi R_{C_4} C_{u_1}}$, $1 = \frac{1}{\chi R C_{u_1}}$ and $p = \frac{0.001}{\chi R C_{u_1}}$ with which we obtain the components values, $R_{C_1} = 16.75k\Omega$, $R_{C_2} = 797619.0476\Omega$, $R_{C_3} = 3988.095238\Omega$, $R_{C_4} = 2M\Omega$, $R_{S_1} = 1k\Omega$ and $R_{S_2} = 13.508k\Omega$. The part of the controller circuit in red box, according to J.C. Sprott [29], simulates the absolute value function while the one in green domains simulates the sign function [30]. The results obtained from these circuits are given in Fig. (20).

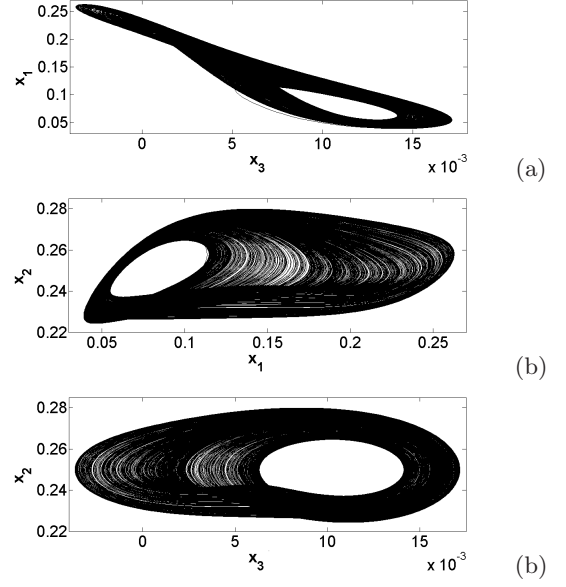


FIG. 16: Chaotic attractor from circuit in Fig. (15)

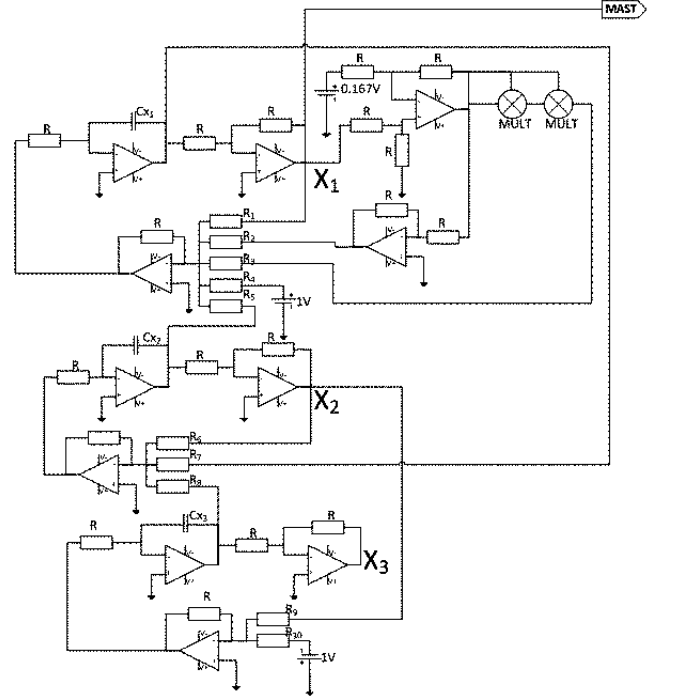


FIG. 17: Circuit diagram of the drive system.

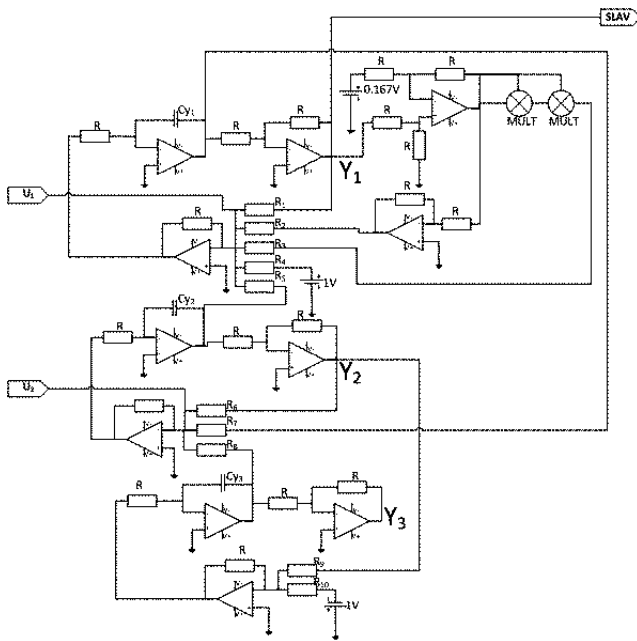


FIG. 18: Circuit diagram of the response system.

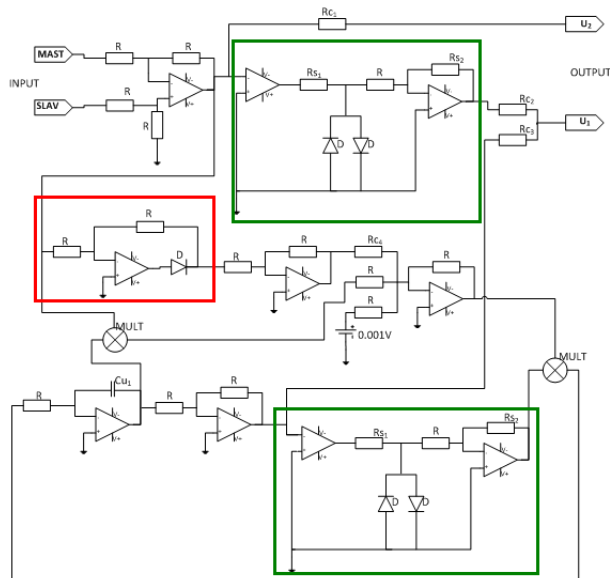


FIG. 19: Circuit diagram of the controller

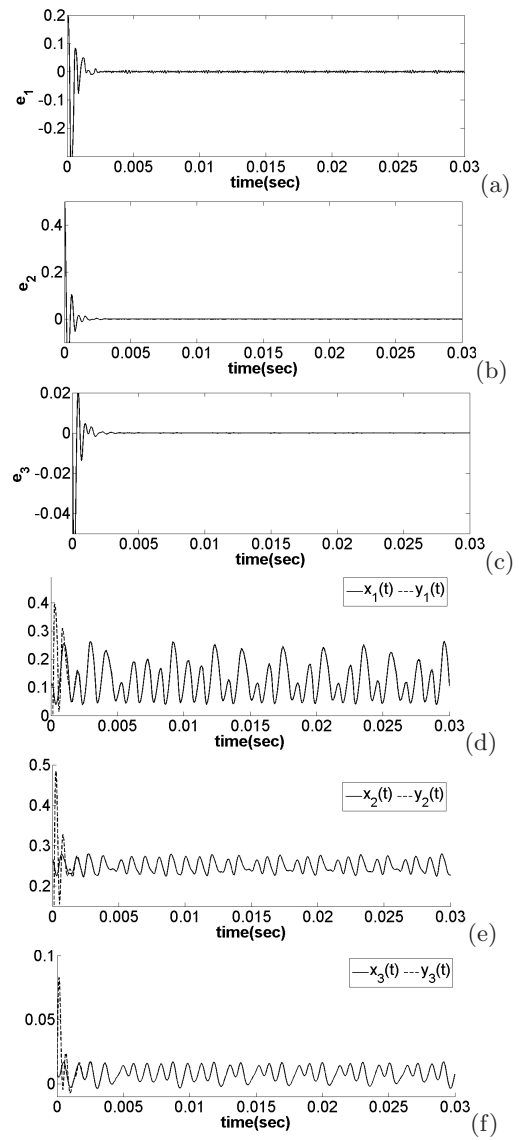


FIG. 20: Time histories of $e_i(t), i = 1, 2, 3$ and of the systems variables.